

## A Cosmic Ray Measurement Facility for ATLAS Muon Chambers

O. Biebel<sup>1</sup>, M. Binder<sup>1</sup>, M. Boutemeur<sup>1</sup>, A. Brandt<sup>1</sup>, J. Dubbert<sup>1</sup>, G. Duceck<sup>1</sup>,  
J. Elmsheuser<sup>1</sup>, F. Fiedler<sup>1</sup>, R. Hertenberger<sup>1</sup>, O. Kortner<sup>2</sup>, T. Nunnemann<sup>1</sup>,  
F. Rauscher<sup>1</sup>, D. Schaile<sup>1</sup>, P. Schieferdecker<sup>1</sup>, A. Staude<sup>1</sup>, W. Stiller<sup>2</sup>,  
R. Ströhmer<sup>1</sup>, and R. Vértési<sup>1</sup>

(1): Ludwig-Maximilians-Universität München,  
Am Coulombwall 1, D-85748 Garching, Germany

(2): Max-Planck-Institut für Physik (Werner-Heisenberg-Institut),  
Föhringer Ring 6, D-80805 München, Germany

### Abstract

Monitored Drift Tube (MDT) chambers will constitute the large majority of precision detectors in the Muon Spectrometer of the ATLAS experiment at the Large Hadron Collider at CERN. For commissioning and calibration of MDT chambers, a Cosmic Ray Measurement Facility is in operation at Munich University. The objectives of this facility are to test the chambers and on-chamber electronics, to map the positions of the anode wires within the chambers with the precision needed for standalone muon momentum measurement in ATLAS, and to gain experience in the operation of the chambers and on-line calibration procedures.

Until the start of muon chamber installation in ATLAS, 88 chambers built at the Max Planck Institute for Physics in Munich have to be commissioned and calibrated. With a data taking period of one day individual wire positions can be measured with an accuracy of  $8.3 \mu\text{m}$  in the chamber plane and  $27 \mu\text{m}$  in the direction perpendicular to that plane.



# 1 Introduction

The large majority of the precision detectors of the muon spectrometer of the ATLAS experiment at the Large Hadron Collider (LHC) will be Monitored Drift Tube (MDT) chambers. These chambers consist of 2 multilayers, each built of 3 or 4 layers of densely packed drift tubes mounted on a support frame made of aluminum (compare figure 1). The drift tubes — which are also made of aluminum — have an outer diameter of 3 cm and a wall thickness of  $400\ \mu\text{m}$ ; in the middle of each tube a gold-plated W-Re anode wire of  $50\ \mu\text{m}$  diameter is stretched. The anode wire is positioned only at the two tube ends by precision end-plugs; the sag of each chamber can be adjusted to follow the sag of the wire along the tube. The drift tubes are operated at a pressure of 3 bar absolute with an Ar:CO<sub>2</sub>=93:7 gas mixture at a gas gain of  $2 \times 10^4$ . The area covered by a complete chamber ranges from  $1\ \text{m}^2$  to  $11\ \text{m}^2$ . A total of 1194 MDT chambers will be used in ATLAS [1].

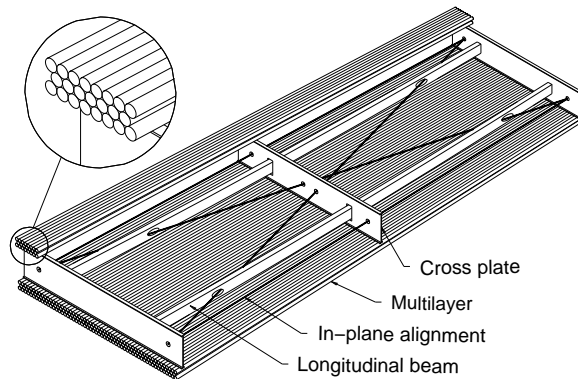


Figure 1: A schematic view of an ATLAS MDT chamber. Also indicated are the optical paths of the geometry monitoring system (in-plane alignment).

In collaboration with the Max Planck Institute (MPI) for Physics, Munich University (LMU) is responsible for the construction of 88 MDT chambers of type BOS (Barrel Outer Small — the second largest type used in the ATLAS barrel region) which consists of 432 drift tubes, arranged in  $2 \times 3$  layers of 72 tubes, and has a size<sup>1</sup> of  $3.9\ \text{m} \times 2.2\ \text{m} \times 0.5\ \text{m}$ . The chambers are built with high mechanical precision at MPI [2] and are then commissioned and calibrated at the Cosmic Ray Measurement Facility of Munich University.

The main objectives of the Cosmic Ray Facility are to test the chambers, to map the positions of the tube layers and of individual anode wires within the chambers, and to gain experience in the operation of the chambers and the calibration procedures.

An important design goal of the ATLAS muon spectrometer is the standalone measurement capability of muon momenta up to 1 TeV with a relative error of less than 10%. This leads to the requirement that the anode wire positions within the MDT chambers must be known to within  $20\ \mu\text{m}$  [1].

## 2 The Cosmic Ray Measurement Facility Setup

A schematic view of the Cosmic Ray Measurement Facility is shown in figure 2. The whole setup is located in a climatized hall to ensure stable environmental

---

<sup>1</sup>Some chambers will be narrower or have cut-outs — realized with shorter drift tubes — to accommodate support structures of the ATLAS detector or feedthroughs to inner components.

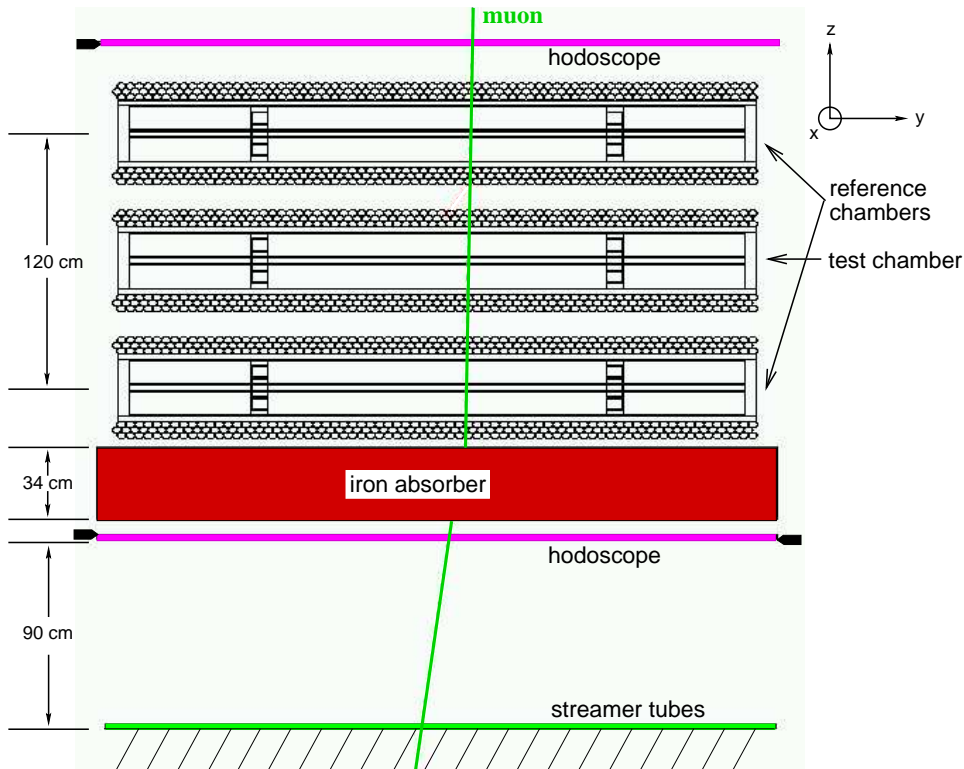


Figure 2: A schematic view of the Cosmic Ray Measurement Facility. The individual components are described in the text.

conditions during the measurements. We define a right handed coordinate system, the  $x$  coordinate in the direction along the wires,  $y$  perpendicular to the wires in the chamber plane, and  $z$  perpendicular to the chamber plane pointing upwards.

Three MDT chambers are operated simultaneously in the facility. Two of them, the so-called reference chambers, encompass the third chamber — which is to be tested — and provide track information for cosmic ray muons. The anode wire positions of the reference chambers have been mapped with a precision of  $2\ \mu\text{m}$  with an X-ray tomograph at CERN [3].

A coincidence of the three scintillator layers in the hodoscopes above and below the MDT chambers provides the trigger. The upper hodoscope consists of one layer of scintillator counters, the lower of two staggered layers displaced by half the width of a counter. Only muons with a momentum greater than  $600\ \text{MeV}$  pass the  $34\ \text{cm}$  iron absorber above the lower hodoscope and can generate a trigger signal. The trigger logic is divided into 5 segments along the  $x$  coordinate to limit the inclination of the muons in the  $x$ - $z$  plane. The arrangement of the scintillator bars allows the measurement of muon tracks in the  $x$  direction with a precision of  $8\ \text{cm}$ . The time of the muon transition is determined by the lower hodoscope with a precision of better than  $800\ \text{ps}$ . The average trigger rate is about  $70\ \text{Hz}$ .

The streamer tubes at the bottom of the setup are used together with the lower reference chamber to determine the multiple scattering angle in the  $y$ - $z$  plane in the iron absorber. This angle is used in combination with the angle between the track segments in the two reference chambers to estimate the momentum of the muon.

Two contact free alignment systems are used to continuously monitor the positions of all MDT chambers: The position of the reference chambers relative to

each other is measured with an optical alignment system consisting of eight RasNik sensors [4], the position of the test chamber with respect to the upper MDT chamber with eight capacitive sensors [5]. Both systems have a precision of better than  $5\ \mu\text{m}$  [6].

In addition to the chamber-to-chamber alignment, the internal chamber geometry is also monitored with integrated RasNik sensors (compare figure 1).

### 3 Drift Time Spectra

The position measurement in the MDT chambers is based on the measurement of the drift time of the electrons (from ionization by the incident muon along its trajectory) to the anode wire. The drift time is determined with respect to the external trigger system and translated to the impact radius (distance from the anode wire) via the so-called  $r$ - $t$  relation (see section 4); the drift tubes are only sensitive to the track coordinates in a plane perpendicular to the anode wire, not along it. The drift of the electrons depends on the gas composition, the gas density, and the electric field applied (i.e. the operating voltage), and is therefore characteristic of the gas mixture and the operating conditions.

After correcting for the signal propagation times along the anode wire and in the electronics and cables, the distributions of drift times are used as a first check that each tube is functioning as expected and that the detector response is homogeneous. For the simple case of uniform illumination of a tube, the density of hits at a given drift time is proportional to the drift velocity at the corresponding radius.

Events with more than one charged particle passing through the setup would lead to ambiguities in the hodoscope time measurement. Therefore, exactly one hit in the upper hodoscope and one pair of hits in overlapping counters in the lower hodoscope are demanded, which rejects 15 % of all triggers (see table 1).

The edges of the drift time spectra are parameterized [7] with the functions

$$F(t) = p_0 + \frac{A_0}{1 + e^{\frac{t_0 - t}{T_0}}} \quad \text{for the rising edge and} \quad (1)$$

$$G(t) = p_m + \frac{\alpha_m t + A_m}{1 + e^{\frac{t - t_m}{T_m}}} \quad \text{for the trailing edge of the spectrum,} \quad (2)$$

as shown in figure 3. The parameters  $p_0$  and  $p_m$  correspond to the rates of accidental hits,  $A_0$  to the height of the spectrum, and  $t_0$  to the mid-time and  $T_0$  to the steepness of the rising edge of the spectrum, which is determined by the resolution of the drift tube near the anode wire. Correspondingly,  $t_m$  is the middle of the trailing edge of the spectrum and  $T_m$  its steepness, which is determined by the decrease in pulse height near the tube wall<sup>2</sup>. The parameterization with  $\alpha_m t + A_m$  accounts for the slope of the spectrum before its trailing edge that is due to the decrease of the drift velocity with increasing radius.

The maximum drift time, defined as  $\tau = (t_m + T_m) - t_0$ , is characteristic of the drift properties of a tube. The distribution of the maximum drift time is shown in figure 4a for the tubes of one MDT chamber. As part of the chamber quality control programme, it is checked that all tubes have the same drift time spectrum characteristics within errors, compare figure 4b.

---

<sup>2</sup>The small pulse height for muons passing a tube close to the tube wall is due to their short path inside the tube, which leads to smaller primary ionization.

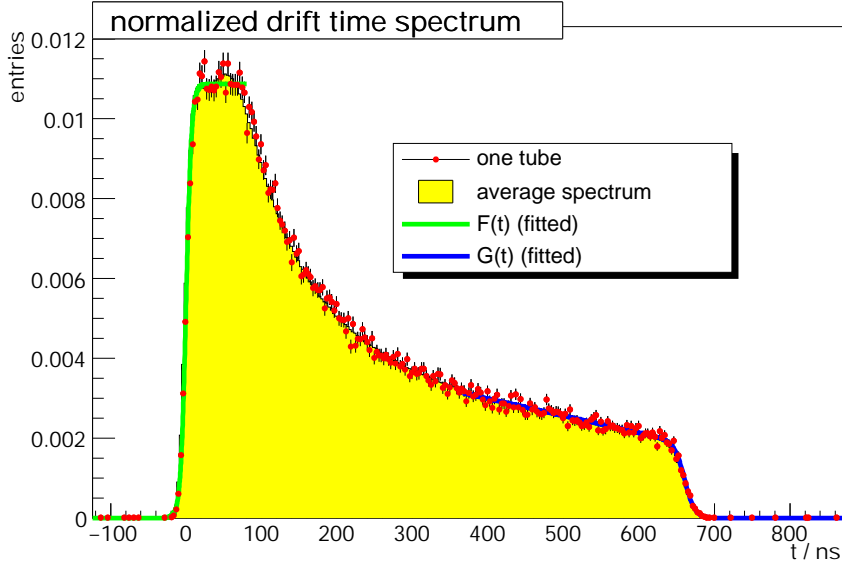


Figure 3: A typical drift time spectrum, normalized to one entry. The fitted functions are explained in the text.

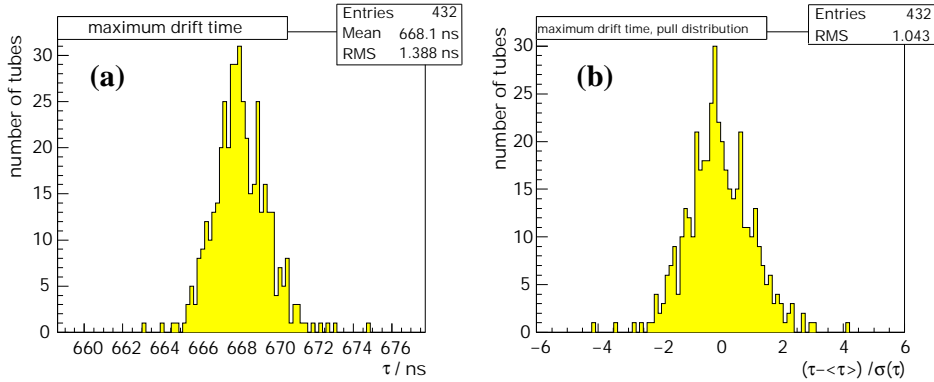


Figure 4: a) Distribution of the maximum drift time  $\tau = (t_m + T_m) - t_0$  for the tubes of a tested chamber. b) The corresponding pull distribution.

## 4 The Relation between Drift Time and Drift Radius

The relation between the measured drift time and the corresponding drift radius ( $r$ - $t$  relation) is determined without the help of external spacial detectors and without assumptions on uniform tube illumination. After the check described in section 3, it is assumed that all tubes of an MDT chamber have the same  $r$ - $t$  relation.

Events with two hits at small drift times ( $|t - t_0| < 15$  ns) in one MDT chamber are selected. By assuming that the muon went through the two corresponding anode wires and that the trajectory of the muon is a straight line, the impact radii

in the other tubes of the chamber can be calculated. This procedure yields drift times for a discrete set of drift radii. The number of such points — typically 16 — is determined by the geometry of the chamber and the angular acceptance of the trigger. In addition to these points, the drift times corresponding to  $r = 0$  and to the inner tube radius are determined by the fit to the drift time spectra described in section 3. The  $r$ - $t$  relation is then approximated by a linear interpolation between the measured values.

## 5 Track Reconstruction

Within each MDT chamber a muon track segment is reconstructed from the measured hits. A track segment is assumed to be a straight line in the  $y - z$  plane<sup>3</sup>:

$$y(z) = m_n z + b_n, \quad (3)$$

where the index  $n$  specifies the chamber. The parameters  $m_n$  and  $b_n$  are determined for each chamber by minimizing the  $\chi^2$  function

$$\chi^2 = \sum_i \frac{(r_{track,i} - r_{drift,i})^2}{\sigma_i(r_{drift,i})^2}, \quad (4)$$

where the index  $i$  runs over all tubes contributing to the track segment,  $r_{track,i}$  is the distance of the track segment to the wire,  $r_{drift,i}$  is the measured drift radius, and  $\sigma_i$  is the resolution of the tube for the given radius. At a test beam measurement using an external reference tracking system of silicon strip detectors the intrinsic single tube resolution was determined to be around  $100 \mu\text{m}$  [8].

The tubes contributing to a track segment are selected by choosing one tube with a hit in each layer of the chamber, which is a sample of six tubes. From the impact radii in the two outermost tubes of this sample four possible track segment candidates are derived. If the difference between the distance of such a candidate to the wire and the measured drift radius does not exceed 2 mm in any of the other tubes, a track segment is fitted using this sample. If more than one track segment is found, the one with the smallest  $\chi^2$  is used. If no track segment is found, the procedure is repeated with subsamples of five tubes.

## 6 Chamber Alignment

The MDT chambers in the Cosmic Ray Facility are aligned mechanically with a precision of about  $100 \mu\text{m}$ . A much more precise estimate of their relative positions is then obtained by comparing the muon track segments reconstructed in each chamber. The optical and capacitive alignment systems are used to verify that the setup does not move significantly during the data taking period. In the future, the alignment information will be included in the analysis to correct for time-dependent position shifts of the chambers.

The positions of the two reference chambers are measured relative to the test chamber.

- A shift  $v_y$  of a reference chamber with respect to the test chamber results in a systematic shift between the track segments in the reference and test chamber and can be obtained from the average over all events,

$$v_y = \langle b_{\text{ref}} - b_{\text{test}} \rangle, \quad (5)$$

---

<sup>3</sup>The third coordinate ( $x$ ) is only used to correct for signal propagation times and for the wire sag and is taken from the hodoscope information.

where  $b_{\text{ref}}$  and  $b_{\text{test}}$  are the track segment parameters defined in equation (3). They are determined with a precision of  $1\ \mu\text{m}$ .

- A shift  $v_z$  results in a relative shift of the track segments depending on the slope  $m$ . It is determined from a linear fit to the distribution of  $b_{\text{ref}} - b_{\text{test}}$  versus  $m$  with an error of  $10\ \mu\text{m}$ .
- A shift  $v_x$  along the  $x$  coordinate can be ignored, as the MDT chambers are not sensitive to such a shift along the direction of their anode wires.
- The tilt angle  $\alpha$  of a reference chamber around the  $x$  axis is given by the systematic deviation of the two track segment slopes as

$$\alpha = \langle m_{\text{ref}} - m_{\text{test}} \rangle . \quad (6)$$

A precision of  $10^{-6}$  is achieved.

- To determine the angles  $\beta$  and  $\gamma$  corresponding to rotations of the reference chamber around the  $y$  and  $z$  axes, the  $x$  coordinate measurement of the hodoscope is used. The shifts  $v_y$  and  $v_z$  are calculated for three one meter wide sections in  $x$ . From the dependences  $v_z(x)$  and  $v_y(x)$ , the angles  $\beta$  and  $\gamma$  are obtained with precisions of  $8 \times 10^{-6}$  and  $10^{-6}$ , respectively.

In the further analysis, the parameters of track segments in the reference chambers are corrected according to the measured reference chamber positions.

## 7 Energy Estimation

The energy of cosmic muons traversing the Cosmic Ray Measurement Facility is estimated from multiple scattering — which depends on the muon momentum — in the chambers and the iron absorber.

If  $m_{\text{ref,u}}$  designates the slope of the track segment reconstructed in the upper reference chamber and  $m_{\text{ref,l}}$  the slope of the track segment reconstructed by the lower reference chamber, the distribution of  $\Delta m = m_{\text{ref,u}} - m_{\text{ref,l}}$  will be the wider the lower the muon energy. The standard deviation  $\sigma_{\Delta m}(E_\mu)$  has been determined as a function of the muon energy by means of a Monte Carlo simulation and can be parameterized as [9]

$$\sigma_{\Delta m}(E_\mu) = \sigma_\infty + \sigma_0 \left( \frac{600\ \text{MeV}}{E_\mu} \right)^\alpha , \quad (7)$$

with  $\sigma_\infty = (2.0 \pm 0.2) \cdot 10^{-4}$ ,  $\sigma_0 = (1.001 \pm 0.008) \cdot 10^{-2}$ , and  $\alpha = 1.04 \pm 0.01$ .

Similarly, the deviation  $\Delta y$  of the position measured with the streamer tubes from the prediction obtained from the track segment in the lower reference chamber depends on the muon energy: For its width  $\sigma_{\Delta y}(E_\mu)$ , a Monte Carlo simulation yields the values  $\sigma_\infty = (4.4 \pm 0.1)\ \text{mm}$ ,  $\sigma_0 = (183 \pm 2)\ \text{mm}$ , and  $\alpha = 1.44 \pm 0.01$ .

The probability density  $f$  for measuring deviations  $\Delta m$  and  $\Delta y$  is then given by

$$f(E_\mu) = \frac{1}{2\pi} \frac{1}{\sigma_{\Delta m}(E_\mu)} \frac{1}{\sigma_{\Delta y}(E_\mu)} \exp \left( -\frac{1}{2} \left[ \left( \frac{\Delta m}{\sigma_{\Delta m}(E_\mu)} \right)^2 + \left( \frac{\Delta y}{\sigma_{\Delta y}(E_\mu)} \right)^2 \right] \right) . \quad (8)$$

For a given track, the value of  $E_\mu$  that maximizes  $f(E_\mu)$  is an estimate of the muon energy. This estimator is biased and has a limited resolution but is still useful for a selection of high momentum muons.

## 8 Measurement of Wire Positions

In this section, the method for the measurement of anode wire positions is presented. To determine wire positions, the muon track segments in the reference chambers

are extrapolated into the test chamber, and the drift radii measured in the test chamber are compared with the track predictions.

The Cosmic Ray Measurement Facility is particularly sensitive to displacements  $\delta y$  of the wires in the chamber plane. From this, a shift of entire tube layers in the  $y$  direction and the mean spacing  $g$  between the wires within a layer can also be determined.

Wire displacements  $\delta z$  in the plane perpendicular to the chamber are accessible via tracks with different inclinations  $m$  (cf. equation (3)). This measurement is less precise than the  $\delta y$  determination owing to the limited angular acceptance of the trigger and the angular distribution of cosmic muons. During chamber production,  $z$  displacement and tilts of entire tube layers are more difficult to control than individual wire displacements  $\delta z$  with respect to the layer. Therefore, the  $z$  displacement for each tube layer is also measured.

The measurements are performed at both ends of the chamber by selecting muons which passed the tested chamber within one meter of the corresponding end of the chamber using the hodoscope information. Because the wires are only supported at the tube ends and since the sag of the anode wires is known from wire tension measurements these two measurements completely determine the wire position.

## 8.1 Event Selection

Events with one reconstructed charged particle are selected as described in section 3. For the further analysis, the event selection proceeds in two steps: First, the reconstructed track segments are subjected to a set of cuts, and second, the individual hits in the tubes must pass certain quality criteria.

The presence of a reconstructed track segment with at least 5 hits is required in each of the three MDT chambers. The track segments must also roughly match, i.e.,  $|b_{\text{ref},u} - b_{\text{ref},l}| < 4 \text{ mm}$  and  $|m_{\text{ref},u} - m_{\text{ref},l}| < 15 \text{ mrad}$ . This ensures that the track segments are not affected by tubes in which delta rays<sup>4</sup> distorted the drift time measurement. The remaining events are called good tracks. For the determination of wire positions, tracks with high muon momentum are desirable to limit the effects from multiple scattering. Thus, the estimated muon energy is required to be larger than 2.5 GeV. The efficiencies of these track cuts are given in table 1.

Tubes in the test chamber with hits generated by delta rays would affect the measurement of the wire position, and are therefore rejected: It is demanded that the tube have contributed to a track segment in the test chamber. Also, a loose cut on the difference between the radius prediction from the reconstructed track segments and the measured drift radius is made. For the track segment reconstructed in the test chamber this cut is at 0.7 mm, while it is at 1.5 mm for the predicted radius from the reference track segments extrapolated into the test chamber<sup>5</sup>. The efficiencies of these cuts are given in table 2. They are very close to 100% and thus do not bias the wire position measurement.

## 8.2 Determination of the Wire Positions

The reconstructed reference chamber track segments are extrapolated into the test chamber and the drift radius measured in the test chamber is compared with the

---

<sup>4</sup>Energetic primary electrons knocked from the tube walls or gas atoms by the incident charged particle. Delta rays can lead to smaller measured drift times if they are emitted in the direction of the anode wire.

<sup>5</sup>The larger value for the reference chamber track segments is due to the long extrapolation distance into the test chamber.



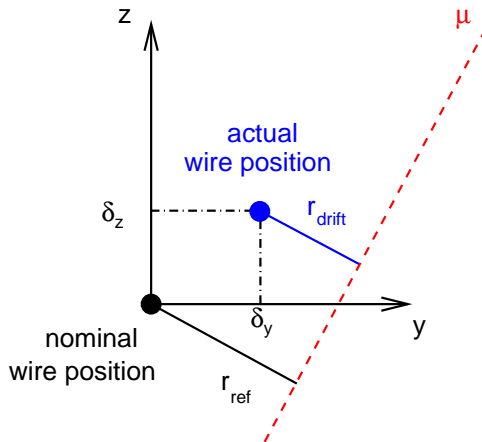


Figure 5: A sketch explaining the method for the measurement of wire displacements. A muon (dashed line) passing a tube with a wire that is displaced from the nominal position by  $\delta y$  in the  $y$  direction and  $\delta z$  in the  $z$  direction will lead to a measured drift radius  $r_{\text{drift}}$ , while  $r_{\text{ref}}$  is predicted by the reference chambers relative to the nominal wire position.

prediction from those track segments. The weighted average  $r_{\text{ref}}$  of the drift radius predictions from the two track segments

$$r_{\text{ref}} = \frac{(1/\sigma_u^2)r_{\text{ref},u} + (1/\sigma_l^2)r_{\text{ref},l}}{(1/\sigma_u^2) + (1/\sigma_l^2)} \quad (9)$$

is taken, where each uncertainty  $\sigma_i$  ( $i = u, l$  for the track segment in the upper and lower reference chamber) depends on the extrapolation distance from the reference chamber and the estimated muon momentum (to account for the uncertainty from multiple scattering). The value of  $\sigma_i$  is about  $200 \mu\text{m}$  for the reference chamber closer to the tube hit and ranges from  $350$  to  $800 \mu\text{m}$  for the farther chamber.

If a given wire is displaced by  $\delta y$  in the  $y$  direction and  $\delta z$  in the  $z$  direction, the measured drift radius  $r_{\text{drift}}$  in the tube will show a systematic deviation  $\Delta r$  from the predicted reference radius,

$$\Delta r = r_{\text{drift}} - r_{\text{ref}} = \delta y - m \delta z + \mathcal{O}(m^2), \quad (10)$$

as shown in figure 5.

### 8.3 Determination of the Wire Position Perpendicular to the Chamber Plane

The displacement  $\delta z$  of an individual anode wire is determined from the slope in a linear fit to the distribution of  $\Delta r$  vs.  $m$ .

The  $z$  displacement of an entire tube layer and its tilt corresponding to a rotation about the  $x$  axis are determined from the distribution of measured  $\delta z$  values of all tubes as a function of their  $y$  coordinate<sup>6</sup>. A linear fit to this  $\delta z$  distribution is performed separately for each layer. The offset and slope of the fitted line are taken to be the  $z$  displacement and tilt of the layer, respectively.

<sup>6</sup>Here,  $y$  is taken to be the nominal wire position. Because of the large chamber width, this approximation does not bias the result.

In the further analysis, each wire is assigned the measured  $z$  position of the layer at the nominal  $y$  wire position. The single wire position measurement is used for wires where it deviates from the layer position by more than 3 standard deviations.

## 8.4 Determination of the Wire Position in the Chamber Plane

Using the  $z$  position measurement described above, the displacement  $\delta y$  of an anode wire is obtained as

$$\langle \Delta r' \rangle = \langle r'_{\text{ref}} - r_{\text{drift}} \rangle = \delta y - \langle m \rangle \delta z' \approx \delta y , \quad (11)$$

where  $r'_{\text{ref}}$  denotes the predicted radius corrected for the wire  $z$  position and the residual displacement  $\delta z'$  after correction is of the order of the resolution of the  $z$  position measurement. The average of the track slopes  $\langle |m|_{\text{all hits}} \rangle_{\text{all tubes}}$  is<sup>7</sup> 0.06, the largest value of  $|m|_{\text{all hits}}$  for a single tube being 0.15. Therefore, the systematic error introduced in the last approximation of equation (11) is typically much smaller than 15% times the resolution on the  $z$  position, which does not limit the  $\delta y$  measurement.

In the chamber plane, the nominal wire positions can be described by a grid of the form

$$y(n) = y_0 + n g , \quad (12)$$

where  $n$  denotes the index of the tube in the layer,  $y_0$  the offset of the layer position relative to the other layers in the same chamber, and  $g$  the mean distance between two neighbouring wires. Fitting the function in equation (12) to the distribution of the wire positions of one tube layer yields the offset  $y_0$  and the mean distance  $g$  for that layer.

## 8.5 Test of the Method

In order to test the method described above, one of the few chambers which have been scanned by the X-ray tomograph at CERN has been used as a test chamber. Two tomograph scans of the chamber were performed at a distance of 30 cm from each chamber end. Therefore the positions of the anode wires<sup>8</sup> are known with a precision of 2  $\mu\text{m}$ .

The analysis uses 28 hours of data taken with this chamber. During this time 1.7 million events per meter along the anode wires ( $x$  direction) have been recorded. The number of events after each step of the event selection and the number of tube hits in the test chamber used for the wire position measurements are given in tables 1 and 2.

All measurements at the Cosmic Ray Facility are in very good agreement with the tomograph results.

In figure 6, the  $\delta z$  measurements for single wires performed at the Cosmic Ray Facility are compared with the results of the tomograph scans. The distributions of the difference between the cosmic ray measurement and the tomograph scan have widths of 23  $\mu\text{m}$  and 27  $\mu\text{m}$ . These widths are dominated by the resolution of the Cosmic Ray Measurement Facility.

A better precision can be obtained for the  $z$  displacement of entire tube layers. A comparison of this measurement and the values for the tilt angle of the tube layers around the  $x$  axis (the parameters which are more difficult to control during the MDT chamber assembly) with the tomograph results is shown in figures 7 and 8.

<sup>7</sup>The deviation from 0 is caused by a slight asymmetry of the trigger efficiency in the  $y$  direction during data taking.

<sup>8</sup>Only typically 80% of the wires are visible in the tomograph scans because of the support structure of the chamber.

selection cut	number of events after cut	efficiency of cut
all events	$1.65 \cdot 10^6$	
hodoscope hits from one particle	$1.40 \cdot 10^6$	85 %
good tracks	$0.84 \cdot 10^6$	60 %
estimated energy $> 2.5$ GeV	$0.34 \cdot 10^6$	40 %

Table 1: Number of events per meter along the wire after each cut in the event selection (second column) and the percentage of events which pass the cut (right column).

selection cut	number of tube hits after cut	efficiency of cut
all tube hits	$2.04 \cdot 10^6$	
hits on tracks	$1.90 \cdot 10^6$	96 %
residuum cuts	$1.87 \cdot 10^6$	98 %

Table 2: Number of tube hits in the test chamber per meter along the wire (as used for the wire position measurement) after each cut in the event selection (second column) and the percentage of hits which pass the cut (right column).

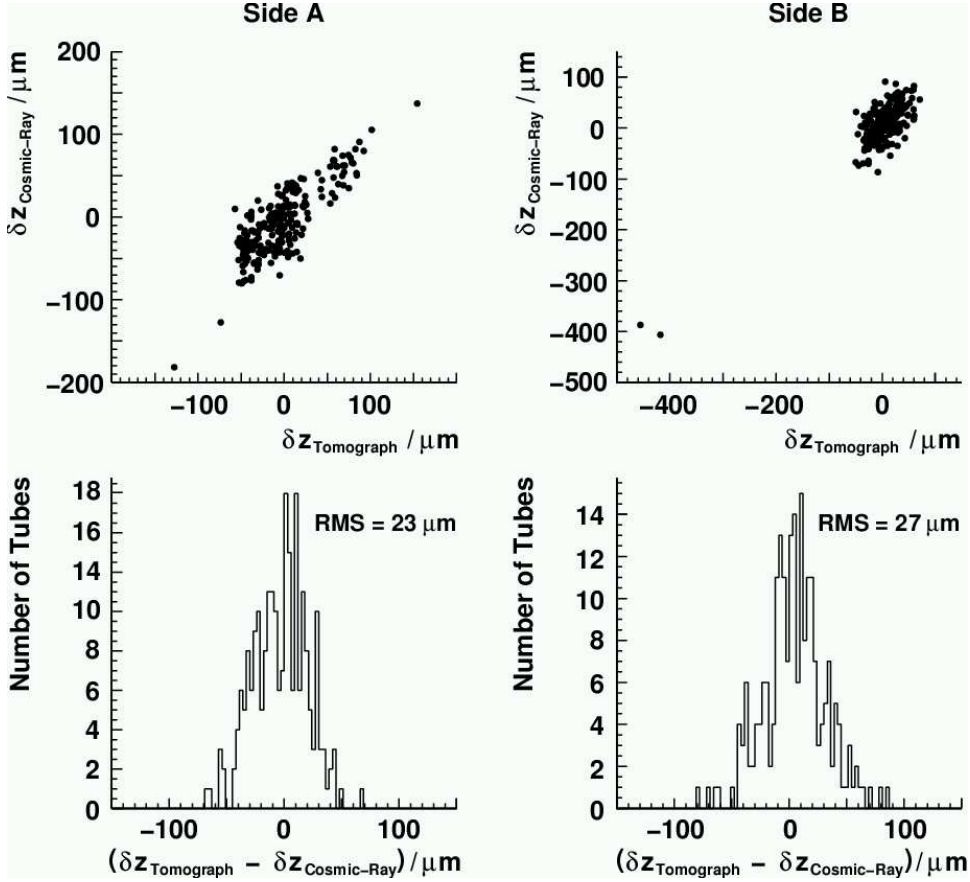


Figure 6: Comparison of the  $\delta z$  measurement for single wires at the Cosmic Ray Facility with the tomograph scans. Note the different scales in the two upper plots.

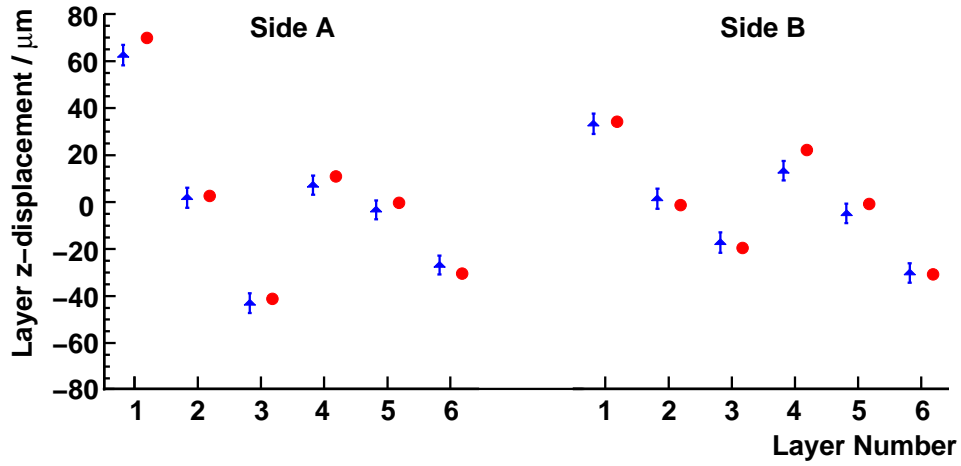


Figure 7: Measurements of  $\delta z$  for entire tube layers. The triangles denote the cosmic ray measurement, the dots the X-ray tomograph data.

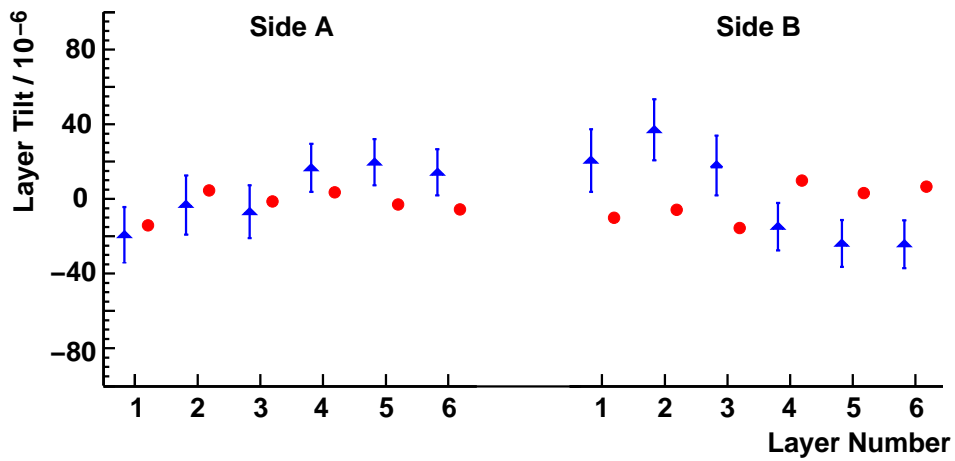


Figure 8: Measurements of the tilt of layers. The triangles denote the cosmic ray measurement, the dots the X-ray tomograph data.

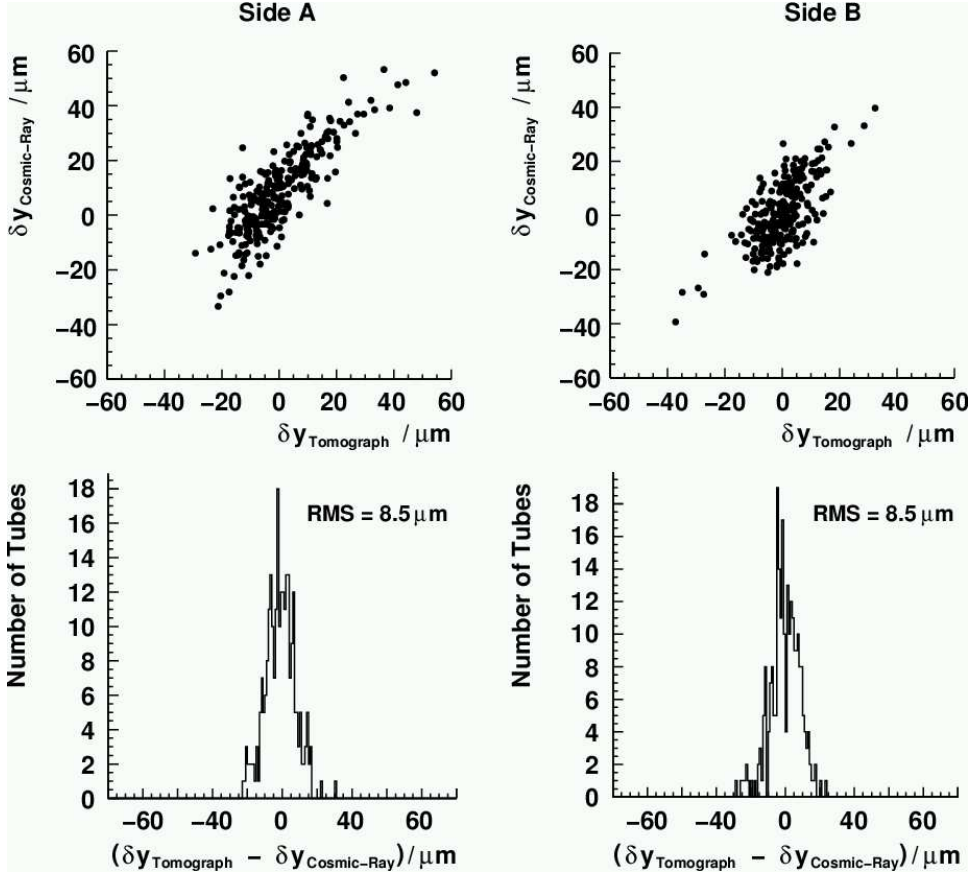


Figure 9: Comparison of the  $\delta y$  measurement for single wires at the Cosmic Ray Facility with the tomograph scans.

Here, we achieve a precision of  $4.4 \mu\text{m}$  for the layer shift and  $17 \times 10^{-6}$  for the tilt angle.

The comparison of the  $\delta y$  measurement with cosmic rays with the tomograph results shows that the difference between the two measurements has an RMS of  $8.5 \mu\text{m}$  at either end of the chamber (see figure 9). The precision of the Cosmic Ray Measurement Facility is therefore  $8.3 \mu\text{m}$  (after subtraction of the uncertainty on the X-ray tomograph measurement).

The measurements of the layer offset  $y_0$  and the wire grid constant  $g$  are compared in figures 10 and 11. A precision of  $1.8 \mu\text{m}$  for the layer offset and  $0.15 \mu\text{m}$  for the grid constant is achieved.

## 9 Conclusions

In the Cosmic Ray Measurement Facility, ATLAS MDT muon chambers are tested and calibrated. The Cosmic Ray Measurement Facility is capable of measuring the positions of the individual anode wires of a chamber with a precision of  $8.3 \mu\text{m}$  in the chamber plane and  $27 \mu\text{m}$  in the direction perpendicular to that plane after 28 hours of data taking.

In addition to the wire positions, the offsets of the tube layers relative to each other in the chamber plane and their grid constants have been determined with

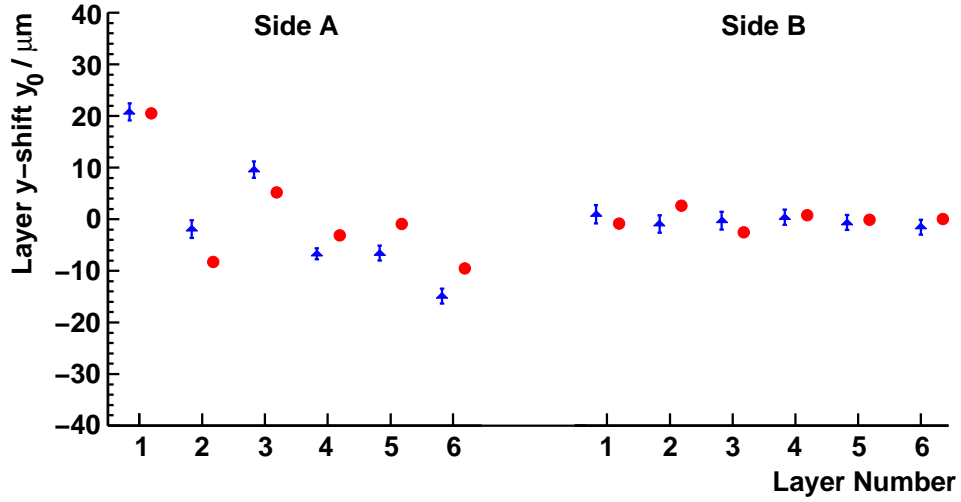


Figure 10: Measurements of the layer shift in  $y$ . The triangles denote the cosmic ray measurement, the dots the X-ray tomograph data.

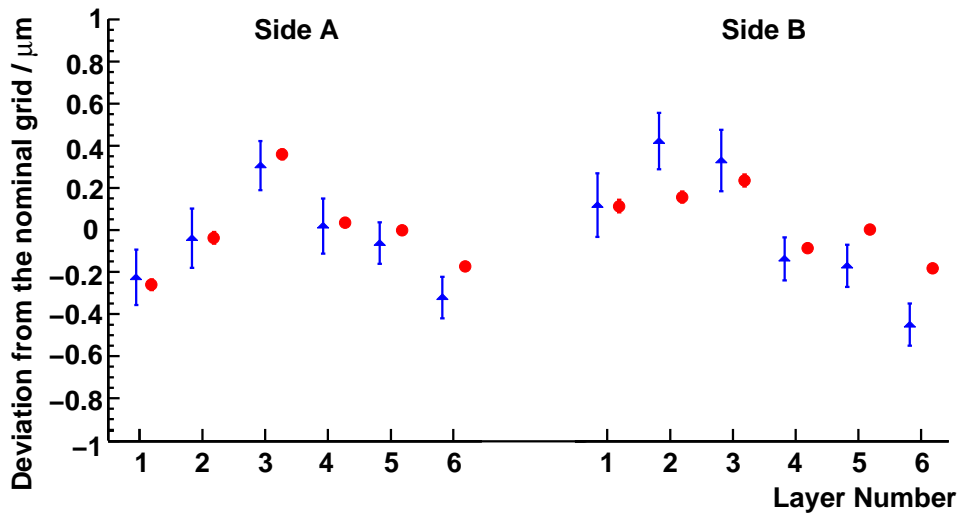


Figure 11: Measurements of the deviation of the grid from the nominal grid. The triangles denote the cosmic ray measurement, the dots the X-ray tomograph data.

precisions of  $1.8\ \mu\text{m}$  and  $0.15\ \mu\text{m}$ , respectively. The positions of the tube layers in the direction perpendicular to the chamber plane and the angles for a rotation around an axis parallel to the wires have been measured with precisions of  $4.4\ \mu\text{m}$  and  $17 \times 10^{-6}$ , respectively.

At a rate of up to two tested chambers per week, all 88 BOS chambers which are produced in Munich will be tested until the planned start of muon chamber installation in ATLAS.

## 10 Acknowledgements

We would like to thank our colleagues at Dubna and MPI Munich for the excellent collaboration, the X-ray tomograph group at CERN for providing their results, and the staff at LMU for their support. We are pleased to acknowledge the support of the Maier-Leibnitz-Laboratorium of LMU and TU Munich, and the Bundesministerium für Bildung und Forschung, Germany.

## References

- [1] The ATLAS Muon Collaboration, *ATLAS Muon Spectrometer Technical Design Report*, CERN/LHCC 97-22, June 1997.
- [2] F. Bauer et al., MPI Report, MPI-PhE/2002-04, October 2002;  
F. Bauer et al., Nucl. Instr. and Meth. A 461 (2001) 17;  
F. Bauer et al., IEEE Trans. Nucl. Sci. 48 (2001) 302.
- [3] J. Berberis et al., *High-precision X-ray tomograph for quality control of the ATLAS muon monitored drift chamber*, Nucl. Instrum. Methods Phys. Res. A 419 (1998) 342-350.
- [4] H. van der Graaf, H. Groenstege, F. Linde, and P. Rewiersma, *RasNiK, an Alignment System for the ATLAS MDT Barrel Muon Chambers - Technical System Description*, NIKHEF/ET38110, 2000.
- [5] S. W. Mackall, *Measurement of the Stability in the Relative Alignment between the Silicon Microvertex Detector and the Time Expansion Chamber Subdetectors in the L3 Experiment at CERN during 1994 Large Electron Positron Collider Run*, Master thesis, Tuscaloosa, 1995.
- [6] A. Kraus, *Genaue Bestimmung der Ereigniszeit und Entwicklung eines Alig-nierungssystems für einen großen Höhenstrahlteststand*, Diploma thesis, LMU Munich, 2001;  
W. Stiller, *Optical and Capacitive Alignment of ATLAS Muon Chambers for Calibration with Cosmic Rays*, Diploma thesis, LMU Munich, 2002.
- [7] O. Kortner and F. Rauscher, *Automatic Synchronization of Drift-Time Spectra and Maximum Drift-Time Measurement of an MDT*, ATLAS internal note ATL-COM-MUON-2002-006, CERN, 2002.
- [8] M. Deile et al., *Resolution and Efficiency Studies with a BOS Monitored Drift-Tube Chamber and a Silicon Telescope at the Gamma Irradiation Facility*, ATLAS internal note, ATL-COM-MUON-2003-006, CERN, 2003.
- [9] O. Kortner, *Schauerproduktion durch hochenergetische Myonen und Aufbau eines Höhenstrahlungsprüfstandes für hochauflösende ATLAS-Myonkammern*, PhD Thesis, LMU Munich, 2002.